Hemilability of phosphine-thioether ligands coordinated to trinuclear Mo$_3$S$_4$ clusters and its effect on hydrogenation catalysis

Artem L. Gushchin,[a,b]* Nikita Y. Shmelev,[a,b] Svetlana F. Malysheva,[c] Alexander V. Artem'ev,[a] Nataliya A. Belogorlova,[c] Pavel A. Abramov,[a] Nikolay B. Kompan'kov,[a] Eric Manoury,[d] Rinaldo Poli,[d] Dmitriy G. Sheven,[a] Rosa Llusar,[e] Maxim N. Sokolov[a,b]

[a] Nikolaev Institute of Inorganic Chemistry, Siberian Branch of the Russian Academy of Sciences, 3 Lavrentiev av., Novosibirsk, 630090, Russia

[b] Novosibirsk State University, 2 Pirogov str., Novosibirsk, 630090, Russia

[c] Favorsky Irkutsk Institute of Chemistry, Siberian Branch of the Russian Academy of Sciences, 1 Favorsky str., Irkutsk, 664033, Russia

[d] Universite de Toulouse, UPS, INPT, 205, route de Narbonne, Toulouse F-31077, France

[e] Departament de Química Física i Analítica, Universitat Jaume I, Av. Sos Baynat s/n, 12071 Castelló, Spain

ABSTRACT

Ligand-exchange reactions of [Mo$_3$S$_4$(tu)$_8$(H$_2$O)]Cl$_4$·4H$_2$O (tu = thiourea) with (PhCH$_2$CH$_2$)$_2$PCH$_2$CH$_2$SR ligands, where R = Ph (**PS1**), pentyl (**PS2**) or Pr (**PS3**) afford new complexes isolated as [Mo$_3$S$_4$Cl$_3$(**PS1**)$_3$]PF$_6$ ([**1**]PF$_6$), [Mo$_3$S$_4$Cl$_3$(**PS2**)$_3$]PF$_6$ ([**2**]PF$_6$) and [Mo$_3$S$_4$Cl$_3$(**PS3**)$_3$]PF$_6$ ([**3**]PF$_6$) salts in 30-50% yields as the major reaction products. The crystal structures of [**1**]PF$_6$ and [**2**]PF$_6$ were determined by X-ray diffraction (XRD) analysis. Each of the three phosphine-thioether ligands is coordinated in a bidentate chelating mode to a different molybdenum atom of the Mo$_3$S$_4$ trinuclear cluster, herewith all the phosphorus atoms of the phosphino-thioether ligand are located *trans* to the capping sulfur (μ$_3$-S). A second product that forms in the reaction of [Mo$_3$S$_4$(tu)$_8$(H$_2$O)]Cl$_4$·4H$_2$O with **PS1** corresponds to the neutral [Mo$_3$S$_4$Cl$_4$(**PS1**)$_2$(**PS1***)] complex. Its XRD analysis reveals both bidentate (**PS1**) and monodentate (**PS1***) coordinating modes of the same ligand. In the latter mode the phosphine-thioether is coordinated to a Mo atom only via the P atom. All compounds were characterized by ^{1}H, ^{31}P{^{1}H} NMR, electrospray-ionization (ESI) mass spectrometry and cyclic voltammetry (CV). Reactions of [**1**]PF$_6$, [**2**]PF$_6$ and [**3**]PF$_6$ with an excess of Bu$_4$NCl in CD$_2$Cl$_2$ were followed by ^{31}P{^{1}H} NMR. The spectra indicate equilibrium between cationic [Mo$_3$S$_4$Cl$_3$(**PSn**)$_3$]$^+$ and neutral [Mo$_3$S$_4$Cl$_4$(**PSn**)$_2$(**PSn***)] (n = 1, 2) species. The equilibrium constants were determined

as $2.5 \pm 0.2 \cdot 10^3$, 43 ± 2 M^{-1} and 30 ± 2 M^{-1} (at 25°C) for [**1**]PF$_6$, [**2**]PF$_6$ and [**3**]PF$_6$, indicating quantitative differences in hemilabile behavior of the phosphino-thioether ligands, depending on the substituent at sulfur. Clusters [**1**]PF$_6$, [**2**]PF$_6$ and [**3**]PF$_6$ were tested as catalysts in reduction of nitrobenzene to aniline with Ph$_2$SiH$_2$ under mild conditions. Significant differencies in the catalytic activity were observed, which can be attributed to different hemilabile behavior of the **PS1** and **PS2/PS3** ligands.

INTRODUCTION

Coordination chemistry of chelating ligands containing mixed functionalities at both coordinating ends has been actively developing in recent decades. In particular, chemistry of the so-called hemilabile ligands, which contain both substitutionally inert and substitutionally labile donor atoms, has received considerable attention.[1-6] The bifunctional character of these polydentate ligands is profitably employed in homogeneous catalysis, small molecule activation by metal complexes, chemical sensing, and stabilization of reactive unsaturated transition metal species.[2-3, 7-33] Important criterion for assigning hemilabile character to a ligand is the reversibility of coordination/decoordination of the labile donor function to/from metal ions.

In contrast to remarkable variety of mononuclear transition metal complexes with hemilabile ligands, the number of polynuclear compounds, and, particularly, metal clusters demonstrating hemilability is still limited.[34-37] Most of the publications in this field deal with carbonyl clusters with heterobidentate ligands, such as phosphine ligands functionalized with sulfur, nitrogen or oxygen atoms, or with a C=C double bond. Different modes of coordination of these ligands to a metal cluster were found. These can be chelating, bridging or monodentate, usually through the phosphorus atom.[38-42]

Our current interest in the field of catalysis is focused on trinuclear chalcogenide molybdenum and tungsten clusters.[43-45] Within the last decade, the groups in Novosibirsk and Castellon have developed synthetic approaches for the functionalization of trinuclear M_3S_4 (M = Mo, W) clusters with homobidentate chelating ligands such as S,S'-donor dithiophosphates,[46-48] P,P'-donor diphosphines,[49-52] N,N'-donor diamines[53-55] or diimines[54, 56-59]. The Mo_3S_4 complexes, functionalized in this way, are excellent chemoselective catalysts for reduction of nitroarenes with different reducing agents.[45, 51, 53-54]

Recently, amino-phosphines were coordinated to the M_3S_4 clusters.[60-62] These heterobidentate ligands are potentially hemilabile, taking into account dual σ-donor and π-acceptor character of the phosphorus atom and only σ-donor properties of nitrogen. Nevertheless, there has been no evidence until now for their hemilabile behavior in M_3S_4 complexes. Furthermore, gas-phase fragmentation of $[Mo_3S_4X_3(edpp)_3]^+$ (X = Cl, Br) complexes {edpp = (2-aminoethyl)diphenylphosphine} with the release of neutral HX molecules and generation of molybdenum/imine Mo=NH species, identified by ESI-MS and supported by DFT calculations, contradicts the assumption of the amino-phosphine ligand hemilability in these clusters.[62] For (P,O)-ligands, the hemilability of hydroxyalkyl diphosphines attached to the M_3S_4 cluster has been demonstrated: depending on the pH of the solution these ligands can act either as bidentate P,P'-donor or tridentate P,P',O-donor ligands.[63-64]

Moreover, it has been reported that the dissociation/reassociation of one of the S atom of the S,S'-donor diethyldithiophosphate ligand most likely plays a key role in the dynamic processes in solutions of Mo_3S_4 complexes of this ligand.[47, 65] A similar mechanism involving partial de-coordination of the P,P'-donor diphosphine in $[Mo_3S_4Cl_3(dppe)_3]^+$ was proposed to explain interconversion between the P-$[Mo_3S_4Cl_3(dppe)_3]^+$ and M-$[Mo_3S_4Cl_3(dppe)_3]^+$ enantiomers. Such de-coordination creates a vacant position at the metal, producing a Lewis acidic site that presumably catalyzes the [(tris(tetrachlorobenzenediolato)phosphate-(V)] (TRISPHAT) anion epimerization.[66] However, this type of homobidentate ligands is not categorized as hemilabile since the metal-donor interactions are not intrinsically different.

In this work bidentate phosphine-thioethers of $(PhCH_2CH_2)_2PCH_2CH_2SR$ (R = phenyl or Ph, **PS1**; pentyl, **PS2**; propyl or Pr, **PS3**) type possessing potentially hemilabile properties[67-68] have been coordinated to the Mo_3S_4 cluster for the first time. The structures of the ligands are depicted in Figure 1.[69] Three complexes were synthesized and characterized as $[Mo_3S_4Cl_3(\textbf{PS1})_3]PF_6$, $[Mo_3S_4Cl_3(\textbf{PS2})_3]PF_6$ and $[Mo_3S_4Cl_3(\textbf{PS3})_3]PF_6$ salts, in which the phosphine-thioether ligands act as bidentate P,S-donors. Interestingly, neutral $[Mo_3S_4Cl_4(\textbf{PS1})_2(\textbf{PS1*})]$ complex containing both PS-bidentate (**PS1**) and P-monodentate (**PS1***) ligands was also isolated. To the best of our knowledge this is the first structurally characterized trinuclear M_3S_4 complex where the same ligand has both monodentate and chelating coordination modes. Equilibrium in solution between cationic $[Mo_3S_4Cl_3(\textbf{PS})_3]^+$ and neutral $[Mo_3S_4Cl_4(\textbf{PS})_2(\textbf{PS*})]$ in the presence of additional chloride anions was observed. The equilibrium constants for the reactions of [**1**]PF_6, [**2**]PF_6 and [**3**]PF_6 with Cl⁻, determined from $^{31}P\{^1H\}$ NMR data, show different hemilabile behavior of the phosphine-thioether ligand depending on the nature of the substituent at the sulfur atom. This leads to marked difference in the catalytic activity of [**1**]PF_6, [**2**]PF_6 and [**3**]PF_6 in the reduction of nitrobenzene to aniline with Ph_2SiH_2.
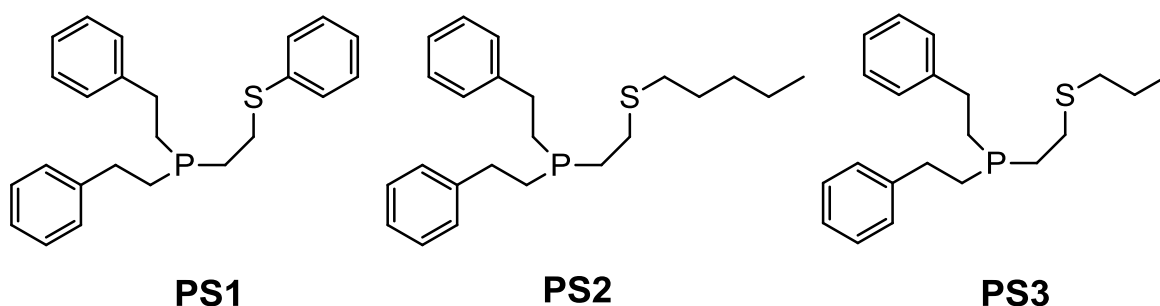

Figure 1. Phosphine-thioether ligands employed in this work[69]

RESULTS AND DISCUSSION

Synthesis and crystal structure

In previous works we have shown that the high lability of the thiourea ligands in easily accessible $[Mo_3S_4(tu)_8(H_2O)]Cl_4 \cdot 4H_2O$ precursor can be used to prepare tri-substituted Mo_3S_4 complexes with 1,10-phenanthroline, 2,2'-bipyridine and its 4,4'-alkyl-substituted derivatives and N,N'-dimethylethylenediamine ligands.[54, 56-57] In this work we used this precursor for ligand-exchange reactions with phosphino-thioethers **PS1**, **PS2** and **PS3** (Figure 1). The target complexes were isolated after purification on a silica-gel chromatographic column and elution with a KPF_6 solution as air-stable [**1**]PF_6, [**2**]PF_6 and [**3**]PF_6 salts in 30-50% yields. Oxygen-free conditions during the reaction are required to prevent oxidation of easy oxidizable phosphine-thioethers. The general synthetic scheme is depicted in Figure 2.
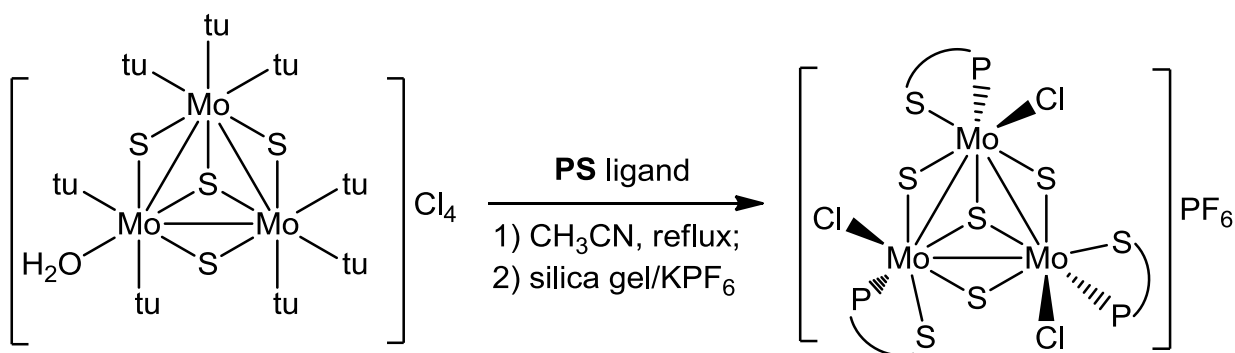

Figure 2. General scheme for preparation of Mo_3S_4 complexes with phosphino-thioether (**PS**) ligands (tu = thiourea)

Single crystals of [**1**]$PF_6 \cdot CH_3CN$ and [**2**]$PF_6 \cdot 0.6CH_3CN$ were obtained by slow evaporation of acetonitrile solutions of the respective complexes. The molecular structure of the $[Mo_3S_4Cl_3(PS1)_3]^+$ cation is shown in Figure 3. Selected bond distances are given in Table 2. The structure consists of an incomplete cuboidal arrangement in which the molybdenum and sulfur atoms occupy adjacent vertices with a missing vertex. Metal–metal and metal–sulfur distances within the Mo_3S_4 cluster core follow the tendencies observed in other trinuclear Mo_3S_4 species.[57, 60] Each molybdenum atom presents a distorted octahedral coordination environment, surrounded by three sulfur ligands, one chlorine, and one phosphorous and one sulfur atoms of the phosphine-thioether ligand, where all the phosphorus atoms are located *trans* to the capping sulfur (μ_3-S). Such preferential spatial disposition of the bifunctional ligand when coordinated to the trinuclear cluster unit is not unprecedented, and also observed in M_3S_4 (M = Mo, W) clusters bearing aminophosphines containing P and N donor atoms.[60-61] The crystal structures of [**1**]PF_6 and [**2**]PF_6 feature intermolecular π-π stacking interactions between C_6H_5 rings of PS ligands (centroid–centroid distance 4.4 Å) (Figure S1).
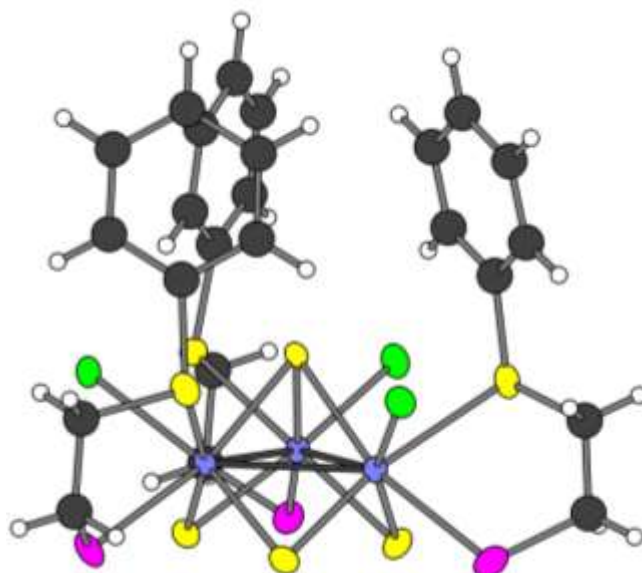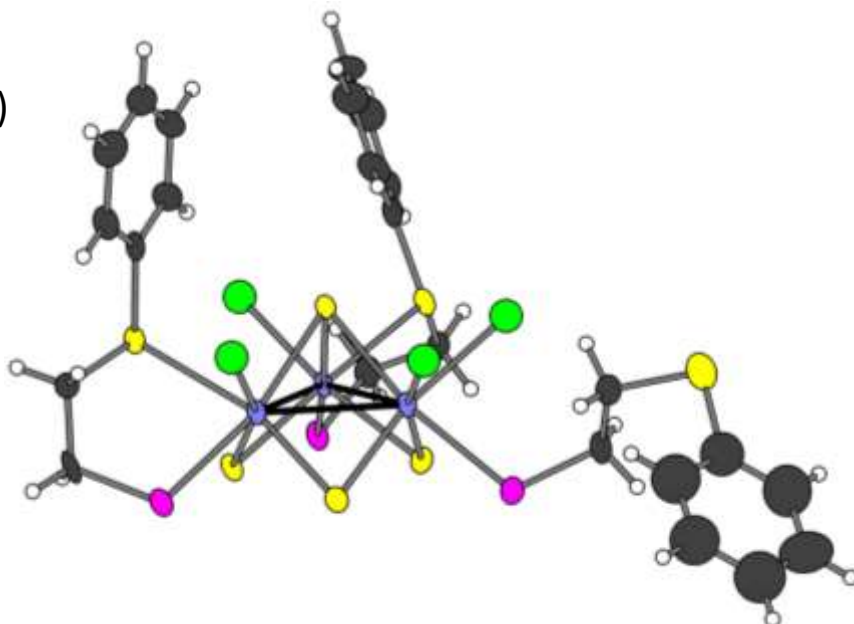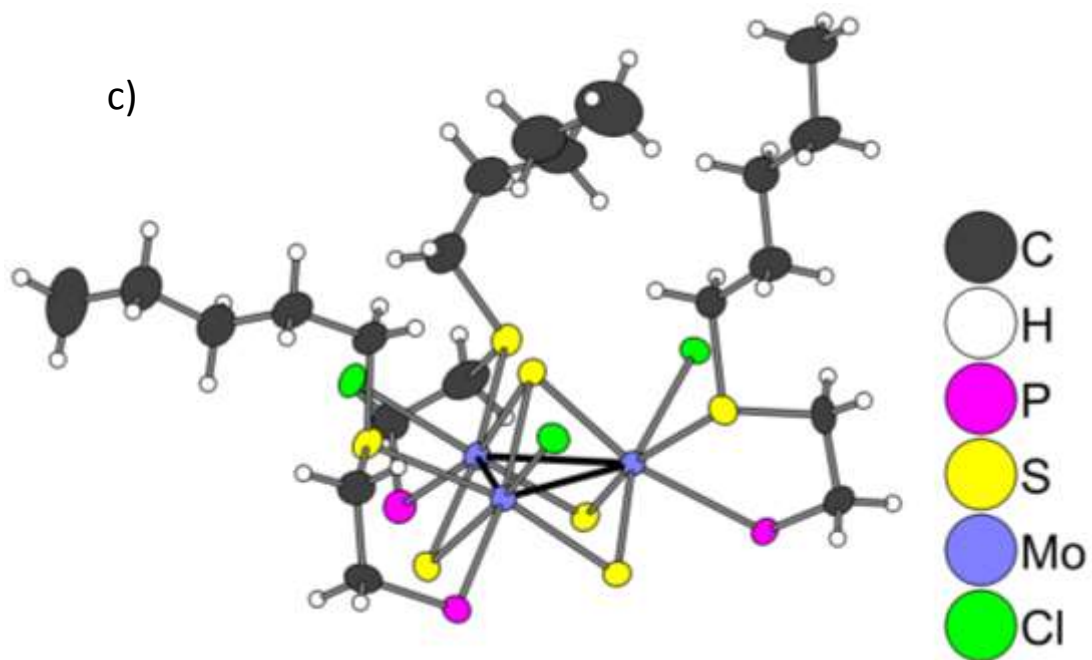
Figure 3. View of XRD-determined structures of cluster complexes of respective compounds [**1**]PF$_6$, [**1a**] and [**2**]PF$_6$: *a)* [Mo$_3$S$_4$Cl$_3$(**PS1**)$_3$]$^+$; *b)* [Mo$_3$S$_4$Cl$_4$(**PS1**)$_2$(**PS1***)]; c) [Mo$_3$S$_4$Cl$_3$(**PS2**)$_3$]$^+$. Substituents at P atoms are omitted for clarity

It is worth noting that the Mo-S distances (2.60-2.66 Å) involving the **PS** ligand S atoms in all complexes are significantly elongated, exceeding by 0.06-0.14 Å the Mo-P bond lengths despite the covalent radius of sulfur being less than that of phosphorus. For comparison, average Mo-S bond length found in labile diethylthiophosphate Mo$_3$S$_4$ complexes is 2.57 Å.[46] The distance between molybdenum and sulfur of the thiourea ligand in [Mo$_3$S$_4$(tu)$_8$(H$_2$O)$_6$]Cl$_4$·4H$_2$O is 2.589(2) Å.[56, 70] All this is consistent with weaker donor ability of the sulfur atoms in phosphine-thioether ligands and their hemilabile behaviour (see below).

The FT-IR spectra of [**1**]PF$_6$, [**2**]PF$_6$ and [**3**]PF$_6$ display the C–H and aromatic C=C stretching vibrations at 2858–3060 and 1528–1604 cm^{-1}, respectively, from the PS ligand. The P–C deformation vibrations overlapped with the CH$_2$ deformation vibrations at 1404–1496 cm^{-1}. The characteristic Mo$_3$-μ_3-S vibration bands are observed in the 444-447 cm^{-1} region.[71] The strong absorption bands at 557 and 837-840 cm^{-1} belong to the P-F vibrations of the PF$_6$ anion.

The structural integrity of [**1**]PF$_6$, [**2**]PF$_6$ and [**3**]PF$_6$ in solution was proven by ^{1}H, ^{31}P{^{1}H} NMR and UV-vis spectroscopies, electrospray-ionization (ESI) mass spectrometry and cyclic voltammetry (CV). ^{31}P{^{1}H} NMR spectra registered in CD$_3$CN reveal a single signal at 38.6 ppm for [**1**]PF$_6$, 40.6 ppm for [**2**]PF$_6$ and 40.4 ppm for [**3**]PF$_6$. This is in agreement with the presence of three equivalent phosphorus nuclei. Electronic absorption spectra of [**1**]PF$_6$, [**2**]PF$_6$ and [**3**]PF$_6$ show absorption bands in the visible part at 618-642 nm which are characteristic for the {Mo$_3$S$_4$} cluster unit.[72-73]

ESI mass spectra of [**1**]PF$_6$, [**2**]PF$_6$ and [**3**]PF$_6$ in CH$_3$CN show one pseudomolecular peak at 1659, 1639 and 1556 m/z associated with [Mo$_3$S$_4$Cl$_3$(**PS1**)$_3$]$^+$, [Mo$_3$S$_4$Cl$_3$(**PS2**)$_3$]$^+$ and [Mo$_3$S$_4$Cl$_3$(**PS3**)$_3$]$^+$ cations, respectively, on the basis of the *m/z* value and characteristic isotope pattern.

Cyclic voltammogram for [**1**]PF$_6$ in CH$_3$CN reveals one reversible reduction at -0.44 V (ΔE = 0.08 V, vs. Ag/AgCl) (Figure S2) and one irreversible reduction process at -1.2 V. This redox behavior is consistent with the literature data and corresponds to the consecutive one-electron Mo$_3^{IV,IV,IV}\rightarrow$Mo$_3^{III,IV,IV}$ and Mo$_3^{III,IV,IV}\rightarrow$Mo$_3^{III,III,IV}$ reductions of the trinuclear cluster core. Other complexes [**2**]PF$_6$ and [**3**]PF$_6$ demonstrate similar redox behavior (see experimental part).

Hemilability of phosphine-thioether ligands

Unexpectedly, in an attempt to isolate the [**1**]Cl salt without treatment with KPF$_6$, diffusion of hexane into a CH$_2$Cl$_2$ solution obtained after removal of thiourea before loading on silica-gel column led to the formation of a mixture of green and brown crystals. The green product is the expected [**1**]Cl salt. The brown product, as revealed by X-ray analysis, is a neutral complex [Mo$_3$S$_4$Cl$_4$(**PS1**)$_2$(**PS1***)]·1.6CH$_2$Cl$_2$ ([**1a**]·1.6CH$_2$Cl$_2$) (Figure 3b) where one of the **PS1** ligands becomes monodentate (**PS1***) and coordinates to the Mo atom through only phosphorous donor atom, demonstrating hemilabile behavior. The coordination left vacant after breaking of the Mo-S bond is occupied by a chloride ligand. The source of Cl$^-$ might be outer-sphere chloride in [**1**]Cl or HCl, which is common impurity in CH$_2$Cl$_2$. The ^{31}P{^{1}H} NMR spectrum of the brown crystals shows two singlets at 37.5 and 37.0 ppm in 2:1 ratio, indicating two types of phosphorous atoms (two P atoms from **PS1** and one from **PS1***). To the best of our knowledge, this is the first structurally characterized trinuclear M$_3$S$_4$ (M = Mo, W) complex demonstrating different dentation modes of the same outer ligand.

During isolation of [**2**]Cl and [**3**]Cl, separation into brown and green components on the chromatographic column was also visible, but the brown product could not be crystallized.

The mixture of [**1**]Cl and [**1a**] was further loaded on a silica-gel column and eluted with a saturated solution of KPF$_6$ in acetone to produce a mixture of [**1**]PF$_6$ and [**1a**]. This mixture was separated by washing with CHCl$_3$ due to low solubility of [**1**]PF$_6$ in CHCl$_3$, to afford a brown filtrate and green powder of analytically pure [**1**]PF$_6$. Unfortunately we were not able to obtain a neutral complex [**1a**] as individual compound following this procedure. The ^{31}P{^{1}H} NMR spectrum of the brown solution after filtration shows signals from [**1a**], [**1**]PF$_6$ and other unidentified species. Remarkably, ESI-MS of this brown solution shows two pseudomolecular peaks centered at m/z = 1659.1 ([**1**]$^+$) and 1698.1. The second one is attributed to the coordination of one CH$_3$CN molecule ([**1**+CH$_3$CN]$^+$) on the basis of the *m/z* value and its characteristic isotope pattern (see Figure S3). This peak cannot be derived from [**1**]$^+$ due to the absence of vacant coordination sites but its formation can be easily explained in terms of the substitution of one chloride in [**1a**] by CH$_3$CN, indirectly confirming the hemilabile behavior of **PS1**.

Prompted by these observations, we followed reaction of [**1**]PF$_6$ with extra Cl$^-$ with ^{31}P{^{1}H} NMR. For this purpose an excess of Bu$_4$NCl (15 mg, 5.5·10^{-5} mole) was added to a solution of [**1**]PF$_6$ in CD$_2$Cl$_2$, (0.7 ml, 7.9·10^{-3} M). A color change from green to brown was immediately observed, indicating generation of [**1a**]. The ^{31}P{^{1}H} NMR spectrum of [**1**]PF$_6$ in CD$_2$Cl$_2$ before adding Bu$_4$NCl shows single signal at 37.4 ppm (Figure 4a). In three hours after addition of Bu$_4$NCl the spectrum shows three overlapping signals: δ_1 = 37.4 ppm from [**1**]$^+$, δ_2 =

36.6 ppm and δ_3 = 36.4 ppm from [**1a**] (Figure 4b). The $\delta_1/\delta_2+\delta_3$ integral ratio, 1.0:4.0, remains constant upon increasing the reaction time up to 24 hours. Thus equilibrium between [**1**]$^+$ and [**1a**] in the presence of Cl$^-$ anions takes place under these conditions (equation 1). The equilibrium constant was calculated as $2.5 \pm 0.2 \cdot 10^3$ M^{-1} (at 25°C). It should also be noted that the resonance lines in the second case (Figure 4b) are much broader than those of [**1**]PF$_6$ without Bu$_4$NCl (Figure 4a), indicating a rapid exchange.
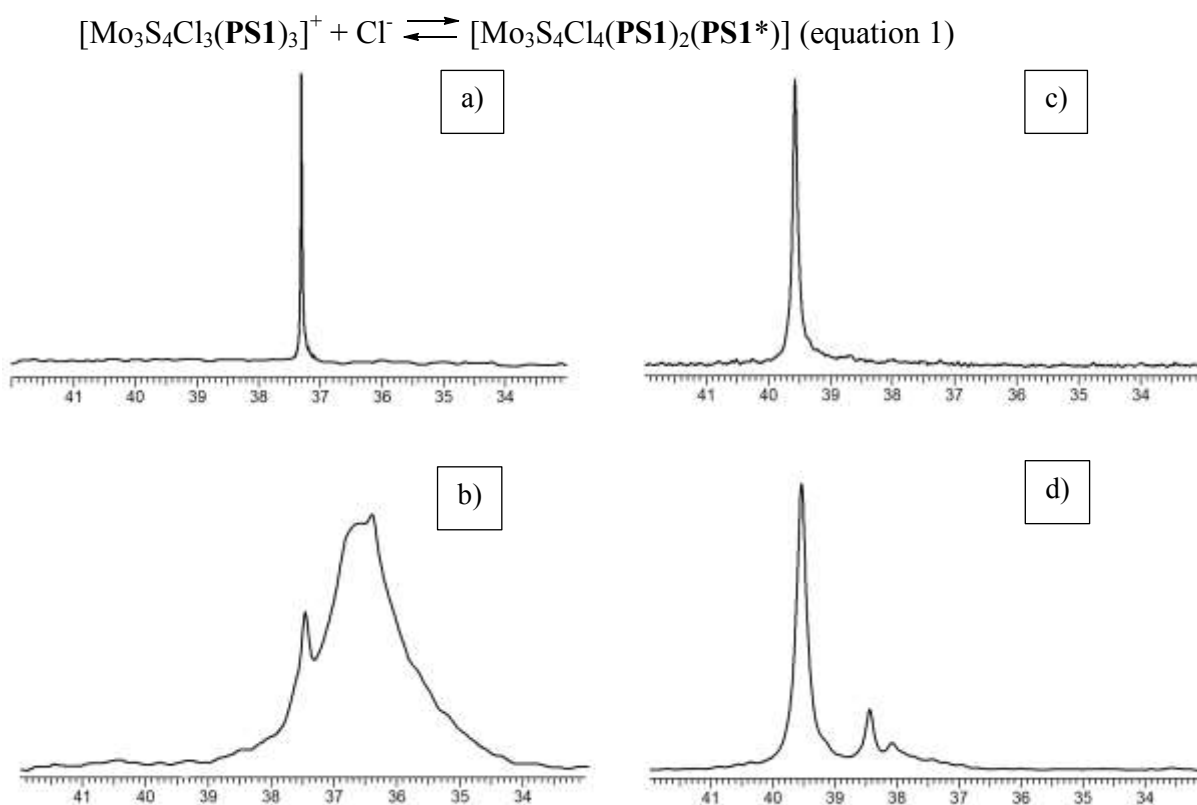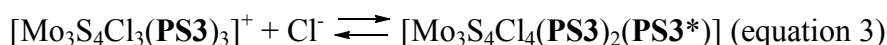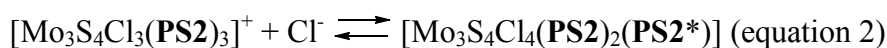
$$[Mo_3S_4Cl_3(\mathbf{PS1})_3]^+ + Cl^- \rightleftharpoons [Mo_3S_4Cl_4(\mathbf{PS1})_2(\mathbf{PS1}^*)] \quad \text{(equation 1)}$$

Figure 4. ^{31}P{^{1}H} NMR spectra: a) [**1**]PF$_6$ before adding of Bu$_4$NCl; b) [**1**]PF$_6$ after three hours of reaction with Bu$_4$NCl; c) [**2**]PF$_6$ before adding of Bu$_4$NCl; d) [**2**]PF$_6$ after three hours of reaction with Bu$_4$NCl

The equilibrium constant was also determined for the reaction of [**2**]$^+$ (c = $8.0 \cdot 10^{-3}$ M) and [**3**]$^+$ (c = $8.0 \cdot 10^{-3}$ M) with Cl$^-$ (equations 2 and 3, respectively) under the same experimental conditions (see spectra in Figure 4 c and d for [**2**]PF$_6$ and Figure S4 for [**3**]PF$_6$): K = 43 ± 2 M^{-1} for [**2**]PF$_6$ (the integral ratio [Mo$_3$S$_4$Cl$_3$(**PS2**)$_3$]$^+$/[Mo$_3$S$_4$Cl$_4$(**PS2**)$_2$(**PS2***)] is 3.7/1.0) and 30 ± 2 M^{-1} for [**3**]PF$_6$ (the integral ratio [Mo$_3$S$_4$Cl$_3$(**PS3**)$_3$]$^+$/[Mo$_3$S$_4$Cl$_4$(**PS3**)$_2$(**PS3***)] is 5.8/1.0). This is 58 and 83 times smaller than that for the reaction of [**1**]$^+$ with Cl$^-$.

$$[Mo_3S_4Cl_3(\mathbf{PS2})_3]^+ + Cl^- \rightleftharpoons [Mo_3S_4Cl_4(\mathbf{PS2})_2(\mathbf{PS2}^*)] \quad \text{(equation 2)}$$
$$[Mo_3S_4Cl_3(\mathbf{PS3})_3]^+ + Cl^- \rightleftharpoons [Mo_3S_4Cl_4(\mathbf{PS3})_2(\mathbf{PS3}^*)] \quad \text{(equation 3)}$$

This difference explains significantly lower amounts of $[Mo_3S_4Cl_4(PS2)_2(PS2^*)]$ and $[Mo_3S_4Cl_4(PS3)_2(PS3^*)]$ observed in the reaction mixtures. The difference in the hemilability between these phosphine-thioether ligands is related to the greater electron-withdrawing properties of the aromatic phenyl group in **PS1** relative to the aliphatic pentyl or propyl group in **PS2** and **PS3**, resulting in a decrease of the sulfur atom σ-donor capacity, weakening the Mo-S bond. This is consistent with the trend in Mo-S_{lig} bond distances (see Table 2). The average values are 2.625 and 2.607 Å for [**1**]PF_6 and [**2**]PF_6, respectively.

Intrigued by the different hemilabile behavior of **PS1** and **PS2/PS3** ligands, we checked how this difference would affect the catalytic activity of [**1**]PF_6, [**2**]PF_6 and [**3**]PF_6 in the benchmark reaction of nitrobenzene reduction to aniline. It was recently shown that Mo_3S_4 clusters functionalized with diphosphane, diamine or diimine ligands catalyze reductions of nitroarenes to anilines with high activity and selectivity.[51, 53-54] In particular, the $[Mo_3S_4Cl_3(dmen)_3](BF_4)$ complex (dmen = N,N'-dimethylethylenediamine) proved effective for reduction of nitroarenes and azocompounds by silanes under mild conditions, to give aromatic amines in good to excellent yields.[53] In this work [**1**]PF_6, [**2**]PF_6 and [**3**]PF_6 were tested as catalysts in the nitrobenzene reduction by diphenylsilane under similar conditions (Figure 5). Gas chromatography (GC) and ^{1}H NMR spectroscopy were used to analyze the reaction products.
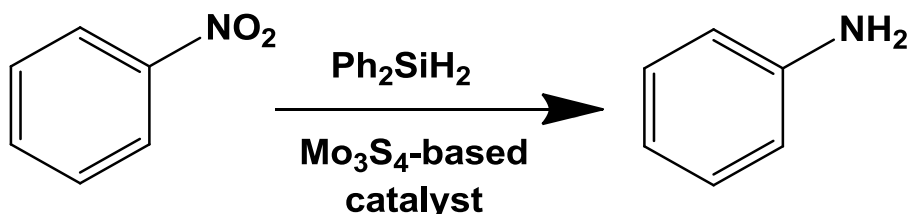

Figure 5. Transformation of nitrobenzene to aniline catalyzed by [**1**]PF_6 or [**2**]PF_6

Table 3 summarizes the results obtained by GC. Full conversion of nitrobenzene and a high yield of aniline (83%) was achieved in CH_3CN as solvent at room temperature in the presence of [**1**]PF_6 (entry 1). In MeOH (which was the most suitable solvent for the catalytic system with $[Mo_3S_4Cl_3(dmen)_3]BF_4)$[53] both the conversion and the yield were significantly lower. Increasing the reaction temperature to 80°C enhances the yield up to >99% (entries 2 and 3). By contrary, [**2**]PF_6 shows less activity under the same conditions (entry 4), and the yield of aniline drops to 33% at room temperature. In all cases except for entry 3, the conversion of nitrobenzene is bigger than the yield of aniline, indicating the presence of possible intermediates of the nitrobenzene reduction. In this regard small amounts of nitrosobenzene and phenylhydroxylamine were detected by ^{1}H NMR at the end of the catalytic reaction for all [**1**]PF_6, [**2**]PF_6 and [**3**]PF_6 (see below). It should be noted that the catalytic system with

[Mo$_3$S$_4$Cl$_3$(dmen)$_3$]BF$_4$ demonstrates higher selectivity at room temperature under similar conditions.[53]

The ^{1}H NMR spectrum recorded in CH$_3$CN/CD$_3$CN mixtures at the end of the catalytic experiment (room temperature, 16 h) reveals full nitrobenzene conversion (>99%) and a 70% yield of aniline for [1]PF$_6$, in agreement with the GC data (entry 1). Complexes [2]PF$_6$ and [3]PF$_6$ show more modest conversions (70 and 50%, respectively) and decreased aniline yields (30 and 24%, respectively) under the same conditions, again in agreement with the GC data for [2]PF$_6$ (entry 4). The difference in the catalytic activity can be attributed to different hemilability between coordinated **PS1** (highly labile) and **PS2/PS3** (moderately labile) ligands, which accounts for the generation of vacant coordination sites and intermediates required for the catalytic reaction. We assume that highly hemilabile **PS1** ligand gives a lower energy span and a higher activity in accordance the Kozuch/Shaik "energy span model".[74-75] Importantly, Mo$_3$S$_4$ clusters with non-hemilabile P,P'-donor diphosphines exhibit less catalytic activity with silanes under similar conditions.[42]

Finally, to check the catalyst integrity throughout the catalytic cycle, ^{31}P{^{1}H} NMR spectra of the reaction mixture were recorded after the catalytic reaction. The presence of one main signal at 48.5 ppm was detected in all cases. It is shifted downfield in comparison with those of [1]PF$_6$ (38.6 ppm), [2]PF$_6$ (40.6 ppm) and [3]PF$_6$ (40.4 ppm) in CD$_3$CN. We believe that this signal still belongs to the [Mo$_3$S$_4$Cl$_3$(**PS**)$_3$]$^+$ species and the shift can be explained by the presence of PhSiH$_2$ in the reaction mixture, which can interact with [Mo$_3$S$_4$Cl$_3$(**PS**)$_3$]$^+$ through the formation of H…Cl hydrogen bonds. This assumption is consistent with the fact that the ESI mass spectra recorded after the catalytic reaction do not reveal the generation of any degradation product (Figure S5). The cluster integrity during catalysis was previously proven for the reduction of nitrobenzene in the presence of the [Mo$_3$S$_4$Cl$_3$(dmen)$_3$]BF$_4$ catalyst monitored by ESI mass spectrometry with a pressurized sample infusion method.[53] This prompts us to assume that the hypothetical Mo-H intermediates generated by silane activation are formed without cleavage of the Mo-Cl bond as found in the analogous Mo$_3$S$_4$ clusters functionalized with diphosphane ligands.[51, 76]

Conclusions

Various phosphine-thioether ligands (**PS**) of "PCH$_2$CH$_2$S" type were coordinated to the trinuclear Mo$_3$S$_4$ cluster for the first time to afford [Mo$_3$S$_4$Cl$_3$(**PS**)$_3$]$^+$ complexes, in which P,S-bidentate coordination mode was observed with a strongly bound P and a more weakly bound S donor atoms. Reversible transformation into neutral [Mo$_3$S$_4$Cl$_4$(**PS**)$_3$(**PS***)] species with P-monodentate ligand (**PS***) in the presence of Cl$^-$ anions was observed and quantified for ligands

PS1, **PS2** and **PS3**. This is in a good agreement with a weaker bonding of the phosphine-thioether ligands sulfur atom, resulting in hemilabile behavior.[67-68] The equilibrium constant between cationic and neutral complexes is strongly depended on the nature of the S atom substituent, with a maximum value for the **PS1** ligands in which the more electron-withdrawing phenyl groups decreases the S atom σ-donating power. This favorable equilibrium shift allowed us to obtain single crystals of the neutral [$Mo_3S_4Cl_4$(**PS1**)$_3$(**PS1***)] complex and determine its crystal structure. This is the first structurally characterized trinuclear M_3S_4 (M = Mo, W) complex showing different dentation modes of the same ligand. Catalytic activity of [**1**]PF_6, [**2**]PF_6 and [**3**]PF_6 in the nitrobenzene reduction by Ph_2SiH_2 reflects the different hemilabile behavior of **PS1** and **PS2/PS3**. Even though the [**1**]PF_6 complex proved less selective than other catalysts based on Mo_3S_4 clusters,[53-54] its catalytic activity in the nitrobenzene reduction is relatively high and higher than that of [**2**]PF_6, [**3**]PF_6 or other Mo_3S_4 complexes with non-hemilabile P,P'-donor diphosphines.[42] This is consistent with the significant hemilabile properties of the phosphine-thioether ligand in [**1**]PF_6, since it can be reversibly decoordinated, generating a coordinating vacancy on the metal atom under mild conditions. Further functionalization of the trimetallic Mo_3S_4 clusters with additional hemilabile ligands may lead to new highly efficient catalytic systems in the future.

EXPERIMENTAL SECTION

General Procedures. All the experiments were carried out under an argon atmosphere using standard Schlenck techniques. The starting complex $[Mo_3S_4(tu)_8(H_2O)]Cl_4 \cdot 4H_2O$ was synthesized according to the published procedure.[56, 70] Phosphine-thioethers were prepared following the literature method.[69] All commercially available reagents (Bu_4NPF_6, KPF_6) were used as purchased. Organic solvents (CH_3CN, CH_2Cl_2, $CHCl_3$ and hexane) were dried by standard methods before use.

Physical Measurements. Elemental C, H, N analyses were performed with a EuroEA3000 Eurovector analyzer. IR spectra were recorded in the 4000–400 cm^{-1} range with a Perkin–Elmer System 2000 FTIR spectrometer with samples in KBr pellets. ^1H and $^{31}P\{^1H\}$ NMR spectra were recorded on a Bruker Avance-500 spectrometer with a 5mm PABBO-PLUS probe at frequencies of 500 (^1H) and 202.46 (^{31}P) MHz at room temperature. The chemical shifts were referenced through ^2D-lock relative to TMS (^1H) and 85% H_3PO_4 (^{31}P). A mass spectrometer (Agilent, 6130 Quadrupole MS, 1260 infinity LC) was used. The drying gas was nitrogen at a 300 L h^{-1} flow rate. The sample solution (approx. $5 \cdot 10^{-5}$ M) in acetonitrile was infused through a syringe pump directly into the interface at a flow rate of 0.4 mL min^{-1}. The temperature of the source block was set to 120 °C and the interface to 150 °C. A capillary voltage of 2.0 kV was used in the positive scan mode, and low values of the cone voltage (Uc = 5-10 V) were used to control the extent of fragmentation. The observed isotopic pattern of each compound perfectly matched the theoretical isotope pattern calculated from their elemental composition by using the MassLynx 4.1 program. The cyclic voltammograms (CV) were recorded with a 797 VA Computrace system (Metrohm, Switzerland). All measurements were performed with a conventional three-electrode configuration consisting of glassy carbon working and platinum auxiliary electrodes and an Ag/AgCl/KCl reference electrode. The solvent used in all experiments was CH_2Cl_2 which was deoxygenated before use. Tetra-n-butylammonium hexafluorophosphate (0.1 M solution) was used as a supporting electrolyte. The concentration of the complexes was approximately 10^{-3} M. The redox potential values ($E_{1/2}$) were determined as ($E_a + E_c$)/2, where E_a and E_c are anodic and cathodic peak potentials, respectively.

Synthesis of $[Mo_3S_4Cl_3(PS1)_3]PF_6$ ([1]PF$_6$). A mixture of $[Mo_3S_4(tu)_8(H_2O)]Cl_4 \cdot 4H_2O$ (0.40 g, 0.32 mmol), bis(2-phenethyl)[2-(phenylsulfanyl)ethyl]phosphine (**PS1**) (0.42 g, 1.1 mmol) and CH_3CN (40 ml) was refluxed for 5 hours. After cooling to room temperature, the resulting suspension was evaporated to dryness. The solid was then extracted with CH_2Cl_2, and the insoluble thiourea excess was removed by filtration. The filtrate was then loaded onto a silica gel column. After washing with CH_2Cl_2, elution with a solution of KPF_6 in acetone (10 mg/mL) afforded a concentrated solution. This solution was evaporated to dryness, the residue extracted

with CH_2Cl_2 and filtered in order to eliminate the inorganic salts. Finally an excess of hexane was layered on the resulting solution. The solid was thoroughly washed with $CHCl_3$ in order to remove impurities including a $[Mo_3S_4Cl_4(PS1)_3(PS1^*)]$ ($[1a]$) neutral complex to afford a green solid of the title compound $[1](PF_6)$. The crystals suitable for X-ray analysis were obtained by slow evaporation of an acetonitrile solution to give $[1](PF_6) \cdot CH_3CN$. Yield: 0.21 g (37 %). Anal. Calc. for $C_{72}H_{81}Cl_3F_6Mo_3P_4S_7$: C, 48.0; H, 4.5%. Found: C, 47.7; H, 4.6%. IR (KBr) cm^{-1}: 3060 (w), 3025 (w), 2953 (m), 2927 (s), 2858 (m), 2042 (w), 1604 (m), 1495 (m), 1453 (m), 1407 (m), 1272 (w), 1211 (w), 1157 (w), 1072 (w), 1002 (w), 958 (w), 840 (s), 739 (s), 698 (s), 557 (m), 494 (w), 444 (w). ^{1}H NMR (500 MHz, 298 K, CD_3CN): δ = 6.77-7.48: (m, 45H, Ph); 2.87-3.02: (m, 6H, C$\underline{H}_2$S); 2.58-2.68: (m, 12H, C$\underline{H}_2$Ph); 1.71-1.79: (m, 18 H, C$\underline{H}_2$P) ppm. ^{31}P$\{^1$H$\}$ NMR (202.46 MHz, 298 K, CD_3CN): δ = 38.6 (s); -144.6 (septet, J^{PF} = 706.6 Hz) ppm. ESI-MS (CH_3CN): m/z: = 1659 ($[Mo_3S_4Cl_3(PS1)_3]^+$). CV (CH_3CN, vs. Ag/AgCl): $E_{1/2}$ = -0.44 V (ΔE = 0.08 V), Ec = -1.2 V at a potential sweep rate of 0.1 V/s. UV/Vis (CH_3CN): $\lambda(\varepsilon)$ = 300 (25070 M^{-1}cm^{-1}), 362 (11250 M^{-1}cm^{-1}), 642 (570 m^{-1}cm^{-1}) nm.

Synthesis of $[Mo_3S_4Cl_3(PS2)_3]PF_6$ ($[2]PF_6$). This compound was prepared in a similar fashion to $[1](PF_6)$, but starting from a mixture of $[Mo_3S_4(tu)_8(H_2O)]Cl_4 \cdot 4H_2O$ (0.38 g, 0.31 mmol), bis(2-phenethyl)[2-(pentylsulfanyl)ethyl]phosphine (**PS2**) (0.40 g, 1.1 mmol) and CH_3CN (40 ml), to give a green solid. The crystals suitable for X-ray analysis were obtained by slow evaporation of acetonitrile solution to give $[2](PF_6) \cdot 0.6CH_3CN$. Yield: 0.25 g (52 %). Anal. Calc. for $C_{69}H_{99}Cl_3F_6Mo_3P_4S_7$: C, 46.4; H, 5.6%. Found: C, 46.2; H, 5.8%. IR (KBr) cm^{-1}: 3058 (m), 3025 (m), 2912 (m), 1956 (w), 1602 (m), 1578 (w), 1496 (m), 1484 (m), 1454 (m), 1440 (m), 1454 (m), 1408 (m), 1254 (w), 1218 (w), 1188 (w), 1157 (w), 1140 (w), 1072 (w), 1026 (w), 1000 (w), 958 (w), 908 (w), 837 (s), 740 (s), 697 (s), 557 (s), 498 (w), 476 (m), 447 (w). ^{1}H NMR (500 MHz, 298 K, CD_3CN): δ = 6.80-7.48 (m, Ph, 30H); 2.84-2.91 (m, 12H, C$\underline{H}_2$Ph); 2.51-2.59: (m, 6H, SC$\underline{H}_2$CH$_2$P); 2.25: (m, 6H, SC$\underline{H}_2$Bu); 1.69-1.73: (m, 18H, C$\underline{H}_2$PC$\underline{H}_2$); 1.56: (m, 6H, C$\underline{H}_2$Pr); 1.36-1.40 (m, 12H, (C$\underline{H}_2$)$_2$Me); 0.95: (m, 9H, C$\underline{H}_3$) ppm. ^{31}P$\{^1$H$\}$ NMR (202.46 MHz, 298 K, CD_3CN): δ = 40.6 (s); -144.6 (septet, J^{PF} = 706.6 Hz) ppm. ESI-MS (CH_3CN): m/z: 1639 ($[Mo_3S_4Cl_3(PS2)_3]^+$). CV (CH_3CN, vs. Ag/AgCl): $E_{1/2}$ = -0.50 V (ΔE = 0.08 V), Ec = -1.3 V at a potential sweep rate of 0.1 V/s. UV/Vis (CH_3CN): $\lambda(\varepsilon)$ = 286 (15180 M^{-1}cm^{-1}), 358 (8530 M^{-1}cm^{-1}), 619 (590 m^{-1}cm^{-1}) nm.

Synthesis of $[Mo_3S_4Cl_3(PS3)_3]PF_6$ ($[3]PF_6$). This compound was prepared in a similar fashion to $[1](PF_6)$, but starting from a mixture of $[Mo_3S_4(tu)_8(H_2O)]Cl_4 \cdot 4H_2O$ (0.52 g, 0.41 mmol), bis(2-phenethyl)[2-(propylsulfanyl)ethyl]phosphine (**PS3**) (0.50 g, 1.4 mmol) and CH_3CN (40 ml), to give a green solid. Yield: 0.33 g (47 %). Anal. Calc. for $C_{63}H_{87}Cl_3F_6Mo_3P_4S_7$: C, 44.5; H, 5.2%. Found: C, 44.2; H, 5.5%. ^{1}H NMR (500 MHz, 298 K, CD_3CN): δ = 6.78-7.54:

(m, 30H, Ph); 2.87-2.95: (m, 12H, C$\underline{H}_2$Ph); 2.40-2.44: (m, 6H, SC$\underline{H}_2$CH$_2$P); 2.20 (m, 6H, SC$\underline{H}_2$Et); 1.90-1.93: (m, 12H, C$\underline{H}_2$PC$\underline{H}_2$); 1.65-1.74 (m, 6H, C$\underline{H}_2$Me); 1.07; (m, 9H, C$\underline{H}_3$) ppm. ^{31}P{^{1}H} NMR (202.46 MHz, 298 K, CD$_3$CN): δ = 40.4 (s); -144.6 (septet, J^{PF} = 706.6 Hz) ppm. ESI-MS (CH$_3$CN): m/z: 1556 ([Mo$_3$S$_4$Cl$_3$(**PS3**)$_3$]$^+$). IR (KBr) cm^{-1}: 3060 (m), 3025 (m), 2961 (m), 2928 (m), 2867 (m), 1602 (w), 1528 (w), 1496 (m), 1454 (m), 1404 (s), 1454 (m), 1410 (m),1340 (w), 1300 (w), 1209 (w), 1058 (w), 1004 (w), 959 (w), 908 (w), 837 (s), 816 (w), 738 (m), 698 (m), 557 (m), 496 (w), 455 (w), 446 (w). CV (CH$_3$CN, vs. Ag/AgCl): E$_{1/2}$ = -0.51 V (ΔE = 0.08 V), Ec = -1.3 V at a potential sweep rate of 0.1 V/s. UV/Vis (CH$_3$CN): $\lambda(\varepsilon)$ = 288 (14220 M^{-1}cm^{-1}), 356 (8600 M^{-1}cm^{-1}), 618 (600 m^{-1}cm^{-1}) nm.

Reaction of [1]PF$_6$ with Bu$_4$NCl. An excess of Bu$_4$NCl (15 mg, 5.5·10^{-5} mol) was added to a solution of [1]PF$_6$ in CD$_2$Cl$_2$, (0.7 ml, 7.9·10^{-3} M). A color change from green to brown was observed. The reaction mixture was stirred at room temperature for up to 24 h and analyzed by ^{31}P{^{1}H} NMR. ^{31}P{^{1}H} NMR (CD$_2$Cl$_2$): δ = 37.4 (s); 36.6 (s); 36.4 (s); -144.6 (septet, J^{PF} = 706.6 Hz) ppm.

Reaction of [2]PF$_6$ with Bu$_4$NCl The reaction was carried out under the same conditions using 15 mg of Bu$_4$NCl (5.5·10^{-5} mol) and a solution of [2]PF$_6$ in CD$_2$Cl$_2$, (0.7 ml, 8.0·10^{-3} M). The reaction mixture was stirred at room temperature for for up to 24 h and analyzed by ^{31}P{^{1}H} NMR. ^{31}P{^{1}H} NMR (CD$_2$Cl$_2$): δ = 39.7 (s); 38.4 (s); 38.2 (s); -144.6 (septet, J^{PF} = 706.6 Hz) ppm.

Reaction of [3]PF$_6$ with Bu$_4$NCl The reaction was carried out under the same conditions using 15 mg of Bu$_4$NCl (5.5·10^{-5} mol) and solution of [3]PF$_6$ in CD$_2$Cl$_2$, (0.7 ml, 8.0·10^{-3} M). The reaction mixture was stirred at room temperature for 24 h and analyzed by ^{31}P{^{1}H} NMR.

^{31}P{^{1}H} NMR (202.46 MHz, 298 K, CD$_2$Cl$_2$): δ = 39.5 (s); 34.0 (s); 32.2 (s); -144.6 (septet, J^{PF} = 706.6 Hz) ppm.

General procedure for nitrobenzene reduction. Nitrobenzene (10 μl, 0.097 mmol), anisole (20 μl) as an internal standard and Ph$_2$SiH$_2$ (3.5 equiv.) were added to a solution of [1]PF$_6$ (9.0 mg, 0.0050 mmol), [2]PF$_6$ (8.9 mg, 0.0050 mmol) or [3]PF$_6$ (8.5 mg, 0.0050 mmol) in deoxygenated CH$_3$CN or CH$_3$CN/CD$_3$CN (2 ml) under an inert atmosphere. The reaction mixture was stirred at room temperature or at 80°C for 16 h. Ethyl acetate (5 ml) was then added, and an aliquot was taken from the resulting solution to be analyzed by GC or ^{1}H NMR.

X-ray data collection and structure refinement. The diffraction data for [1a] (Bruker X8 Apex diffractometer with MoKα radiation), [1]PF$_6$ and [2]PF$_6$ (Bruker Apex Duo diffractometer with MoKα radiation) were collected by doing φ and ω scans of narrow (0.5°) frames at 150 K. Absorption correction was done empirically using SADABS.[77] Crystallographic data and refinement details are given in Table 1. The main bond distances are summarized in Table 2.

Structures were solved by direct method and refined by full-matrix least-squares treatment against $|F|^2$ in anisotropic approximation with SHELX 2017/1 in ShelXle program.[78-79] Hydrogen atoms were refined in geometrically calculated positions. The crystallographic data have been deposed in the Cambridge Crystallographic Data Centre under the deposition codes CCDC 1816782, 1816783, and 1816784.

References

[1]   R. Lindner, B. van den Bosch, M. Lutz, J. N. H. Reek, J. I. van der Vlugt, *Organometallics* 2011, *30*, 499-510.

[2]   C. S. Slone, D. A. Weinberger, C. A. Mirkin, in *Progress in Inorganic Chemistry, Vol 48, Vol. 48* (Ed.: K. D. Karlin), John Wiley & Sons Inc, Hoboken, 1999, pp. 233-350.

[3]   A. Bader, E. Lindner, *Coord. Chem. Rev.* 1991, *108*, 27-110.

[4]   P. Braunstein, F. Naud, *Angew. Chem.-Int. Edit.* 2001, *40*, 680-699.

[5]   J. C. Jeffrey, T. B. Rauchfuss, *Inorg. Chem.* 1979, *18*, 2658-2666.

[6]   M. Bierenstiel, E. D. Cross, *Coord. Chem. Rev.* 2011, *255*, 574-590.

[7]   E. Piras, F. Lang, H. Ruegger, D. Stein, M. Worle, H. Grutzmacher, *Chem.-Eur. J.* 2006, *12*, 5849-5858.

[8]   Z. Q. Weng, S. H. Teo, T. S. A. Hor, *Accounts Chem. Res.* 2007, *40*, 676-684.

[9]   M. Nandi, J. Jin, T. V. RajanBabu, *J. Am. Chem. Soc.* 1999, *121*, 9899-9900.

[10]   Z. Q. Weng, S. Teo, T. S. A. Hor, *Organometallics* 2006, *25*, 4878-4882.

[11]   H. V. Huynh, C. H. Yeo, Y. X. Chew, *Organometallics* 2010, *29*, 1479-1486.

[12]   J. Andrieu, J. M. Camus, P. Richard, R. Poli, L. Gonsalvi, F. Vizza, M. Peruzzini, *Eur. J. Inorg. Chem.* 2006, 51-61.

[13]   A. Acosta-Ramirez, M. Munoz-Hernandez, W. D. Jones, J. J. Garcia, *Organometallics* 2007, *26*, 5766-5769.

[14]   P. Espinet, K. Soulantica, *Coord. Chem. Rev.* 1999, *193-5*, 499-556.

[15]   G. Dekker, A. Buijs, C. J. Elsevier, K. Vrieze, P. Vanleeuwen, W. J. J. Smeets, A. L. Spek, Y. F. Wang, C. H. Stam, *Organometallics* 1992, *11*, 1937-1948.

[16]   P. J. W. Deckers, B. Hessen, J. H. Teuben, *Angew. Chem.-Int. Edit.* 2001, *40*, 2516-+.

[17] P. Braunstein, *J. Organomet. Chem.* 2004, *689*, 3953-3967.

[18] M. Kuriyama, K. Nagai, K. Yamada, Y. Miwa, T. Taga, K. Tomioka, *J. Am. Chem. Soc.* 2002, *124*, 8932-8939.

[19] N. J. Hovestad, E. B. Eggeling, H. J. Heidbuchel, J. Jastrzebski, U. Kragl, W. Keim, D. Vogt, G. van Koten, *Angew. Chem.-Int. Edit.* 1999, *38*, 1655-1658.

[20] M. V. Jimenez, J. J. Perez-Torrente, M. I. Bartolome, V. Gierz, F. J. Lahoz, L. A. Oro, *Organometallics* 2008, *27*, 224-234.

[21] H. Yang, M. AlvarezGressier, N. Lugan, R. Mathieu, *Organometallics* 1997, *16*, 1401-1409.

[22] G. L. Moxham, H. E. Randell-Sly, S. K. Brayshaw, R. L. Woodward, A. S. Weller, M. C. Willis, *Angew. Chem.-Int. Edit.* 2006, *45*, 7618-7622.

[23] W. H. Zhang, S. W. Chien, T. S. A. Hor, *Coord. Chem. Rev.* 2011, *255*, 1991-2024.

[24] C. Muller, R. J. Lachicotte, W. D. Jones, *Organometallics* 2002, *21*, 1975-1981.

[25] A. Ros, B. Estepa, R. Lopez-Rodriguez, E. Alvarez, R. Fernandez, J. M. Lassaletta, *Angew. Chem.-Int. Edit.* 2011, *50*, 11724-11728.

[26] V. Gomez-Benitez, R. A. Toscano, D. Morales-Morales, *Inorg. Chem. Commun.* 2007, *10*, 1-6.

[27] D. Morales-Morales, R. Redon, Y. F. Zheng, J. R. Dilworth, *Inorg. Chim. Acta* 2002, *328*, 39-44.

[28] D. Morales-Morales, S. Rodriguez-Morales, J. R. Dilworth, A. Sousa-Pedrares, Y. F. Zheng, *Inorg. Chim. Acta* 2002, *332*, 101-107.

[29] V. Gomez-Benitez, S. Hernandez-Ortega, D. Morales-Morales, *Inorg. Chim. Acta* 2003, *346*, 256-260.

[30] J. G. Fierro-Arias, R. Redon, J. J. Garcia, S. Hernandez-Ortega, R. A. Toscano, D. Morales-Morales, *J. Mol. Catal. A-Chem.* 2005, *233*, 17-27.

[31] D. Canseco-Gonzalez, V. Gomez-Benitez, S. Hernandez-Ortega, R. A. Toscano, D. Morales-Morales, *J. Organomet. Chem.* 2003, *679*, 101-109.

[32] S. Ramirez-Rave, F. Estudiante-Negrete, R. A. Toscano, S. Hernandez-Ortega, D. Morales-Morales, J. M. Grevy, *J. Organomet. Chem.* 2014, *749*, 287-295.

[33] V. Gomez-Benitez, H. Valdes, S. Hernandez-Ortega, J. M. German-Acacio, D. Morales-Morales, *Polyhedron* 2018, *143*, 144-148.

[34] P. Braunstein, M. Knorr, C. Stern, *Coord. Chem. Rev.* 1998, *178*, 903-965.

[35] N. Lugan, F. Laurent, G. Lavigne, T. P. Newcomb, E. W. Liimatta, J. J. Bonnet, *J. Am. Chem. Soc.* 1990, *112*, 8607-8609.

[36]   N. Lugan, F. Laurent, G. Lavigne, T. P. Newcomb, E. W. Liimatta, J. J. Bonnet, *Organometallics* 1992, *11*, 1351-1363.

[37]   O. Baldovino-Pantaleon, G. Rios-Moreno, R. A. Toscano, D. Morales-Morales, *J. Organomet. Chem.* 2005, *690*, 2880-2887.

[38]   T. M. Rasanen, S. Jaaskelainen, T. A. Pakkanen, *J. Organomet. Chem.* 1998, *553*, 453-461.

[39]   J. D. King, M. Monari, E. Nordlander, *J. Organomet. Chem.* 1999, *573*, 272-278.

[40]   A. J. Deeming, M. K. Shinhmar, A. J. Arce, Y. De Sanctis, *J. Chem. Soc.-Dalton Trans.* 1999, 1153-1159.

[41]   S. P. Tunik, I. O. Koshevoy, A. J. Poe, D. H. Farrar, E. Nordlander, M. Haukka, T. A. Pakkanen, *Dalton Trans.* 2003, 2457-2467.

[42]   D. V. Krupenya, S. I. Selivanov, S. P. Tunik, M. Haukka, T. A. Pakkanen, *Dalton Trans.* 2004, 2541-2549.

[43]   M. N. Sokolov, V. P. Fedin, A. G. Sykes, in *Comprehensive Coordination Chemistry II, Vol. 4* (Eds.: J. A. McCleverty, T. J. Meyer), Elsevier Ltd., Amsterdam, 2004, pp. 761-823.

[44]   V. Y. Fedorov, Y. V. Mironov, N. G. Naumov, M. N. Sokolov, V. P. Fedin, *Uspekhi Khimii* 2007, *76*, 571-595.

[45]   A. L. Gushchin, Y. A. Laricheva, M. N. Sokolov, R. Llusar, *RUSS CHEM REV* 2018, *87*, 670-706.

[46]   R. Hernandez-Molina, A. Gushchin, J. Gonzalez-Platas, M. Martinez, C. Rodriguez, C. Vicent, *Dalton Trans.* 2013, *42*, 15016-15027.

[47]   A. L. Gushchin, R. Hernandez-Molina, A. V. Anyushin, M. R. Gallyamov, J. Gonzalez-Platas, N. K. Moroz, M. N. Sokolov, *New J. Chem.* 2016, *40*, 7612-7619.

[48]   A. L. Gushchin, Y. A. Laricheva, D. A. Piryazev, M. N. Sokolov, *Russ. J. Coord. Chem.* 2014, *40*, 5-9.

[49]   R. Llusar, S. Uriel, *Eur. J. Inorg. Chem.* 2003, 1271-1290.

[50]   T. F. Beltran, M. Feliz, R. Llusar, J. A. Mata, V. S. Safont, *Organometallics* 2011, *30*, 290-297.

[51]   I. Sorribes, G. Wienhöfer, C. Vicent, K. Junge, R. Llusar, M. Beller, *Angewandte Chemie International Edition* 2012, *51*, 7794-7798.

[52]   F. Estevan, M. Feliz, R. Llusar, J. A. Mata, S. Uriel, *Polyhedron* 2001, *20*, 527-535.

[53]   E. Pedrajas, I. Sorribes, K. Junge, M. Beller, R. Llusar, *ChemCatChem* 2015, *7*, 2675-2681.

[54] E. Pedrajas, I. Sorribes, A. L. Gushchin, Y. A. Laricheva, K. Junge, M. Beller, R. Llusar, *ChemCatChem* 2017, *9*, 1128-1134.

[55] E. Pedrajas, I. Sorribes, K. Junge, M. Beller, R. Llusar, *Green Chem.* 2017, *19*, 3764-3768.

[56] A. L. Gushchin, Y. A. Laricheva, P. A. Abramov, A. V. Virovets, C. Vicent, M. N. Sokolov, R. Llusar, *Eur. J. Inorg. Chem.* 2014, 4093-4100.

[57] J. A. Pino-Chamorro, Y. A. Laricheva, E. Guillamon, M. J. Fernandez-Trujillo, E. Bustelo, A. L. Gushchin, N. Y. Shmelev, P. A. Abramov, M. N. Sokolov, R. Llusar, M. G. Basallote, A. G. Algarra, *New J. Chem.* 2016, *40*, 7872-7880.

[58] J. A. Pino-Chamorro, Y. A. Laricheva, E. Guillamon, M. J. Fernandez-Trujillo, A. G. Algarra, A. L. Gushchin, P. A. Abramov, E. Bustelo, R. Llusar, M. N. Sokolov, M. G. Basallotet, *Inorg. Chem.* 2016, *55*, 9912-9922.

[59] Y. A. Laricheva, A. L. Gushchin, P. A. Abramov, M. N. Sokolov, *Polyhedron* 2018, *154*, 202-208.

[60] C. Alfonso, M. Feliz, V. S. Safont, R. Llusar, *Dalton Trans.* 2016, *45*, 7829-7835.

[61] T. F. Beltran, J. A. Pino-Chamorro, M. J. Fernandez-Trujillo, V. S. Safont, M. G. Basallote, R. Llusar, *Inorg. Chem.* 2015, *54*, 607-618.

[62] T. F. Beltran, V. S. Safont, R. Llusar, *Eur. J. Inorg. Chem.* 2016, 5171-5179.

[63] T. F. Beltrán, R. Llusar, M. N. Sokolov, M. G. Basallote, M. J. Fernández-Trujillo, J. Á. Pino-Chamorro, *Inorg. Chem.* 2013, *52*, 8713-8722.

[64] M. G. Basallote, M. Jesus Fernandez-Trujillo, J. Angel Pino-Charnorro, T. F. Beltran, C. Corao, R. Llusar, M. Sokolov, C. Vicent, *Inorg. Chem.* 2012, *51*, 6794-6802.

[65] R. Hernandez-Molina, J. Gonzalez-Platas, K. A. Kovalenko, M. N. Sokolov, A. V. Virovets, R. Llusar, C. Vicent, *Eur. J. Inorg. Chem.* 2011, 683-693.

[66] R. Frantz, E. Guillamon, J. Lacour, R. Llusar, V. Polo, C. Vicent, *Inorg. Chem.* 2007, *46*, 10717-10723.

[67] J. R. Dilworth, N. Wheatley, *Coord. Chem. Rev.* 2000, *199*, 89-158.

[68] R. D. Kennedy, C. W. Machan, C. M. McGuirk, M. S. Rosen, C. L. Stern, A. A. Sarjeant, C. A. Mirkin, *Inorg. Chem.* 2013, *52*, 5876-5888.

[69] B. A. Trofimov, N. K. Gusarova, S. F. Malysheva, N. I. Ivanova, B. G. Sukhov, N. A. Belogorlova, V. A. Kuimov, *Synthesis* 2002, 2207-2210.

[70] Y. A. Laricheva, A. L. Gushchin, P. A. Abramov, M. N. Sokolov, *J. Struct. Chem.* 2016, *57*, 962-969.

[71] V. P. Fedin, Y. V. Mironov, M. N. Sokolov, B. A. Kolesov, V. Y. Fedorov, D. S. Yufit, Y. T. Struchkov, *Inorg. Chim. Acta* 1990, *174*, 275-282.

[72] D. M. Saysell, V. P. Fedin, G. J. Lamprecht, M. N. Sokolov, A. G. Sykes, *Inorg. Chem.* 1997, *36*, 2982-2987.

[73] A. L. Gushchin, B. L. Ooi, P. Harris, C. Vicent, M. N. Sokolov, *Inorg. Chem.* 2009, *48*, 3832-3839.

[74] S. Kozuch, S. Shaik, *Accounts Chem. Res.* 2011, *44*, 101-110.

[75] R. Poli, *Comments Inorganic Chem.* 2009, *30*, 177-228.

[76] A. G. Algarra, M. G. Basallote, M. J. Fernandez-Trujillo, M. Feliz, E. Guillamon, R. Llusar, I. Sorribes, C. Vicent, *Inorg. Chem.* 2010, *49*, 5935-5942.

[77] G. M. Sheldrick, *University of Göttingen, Germany* 1996.

[78] G. M. Sheldrick, *Acta Crystallogr. Sect. A* 2015, *71*, 3-8.

[79] C. B. Hubschle, G. M. Sheldrick, B. Dittrich, *J. Appl. Crystallogr.* 2011, *44*, 1281-1284.

GRAPHICAL ABSTRACT

Phosphine-thioether ligands **PS1**, **PS2** and **PS3** were coordinated to the trinuclear Mo_3S_4 cluster for the first time to afford $[Mo_3S_4Cl_3(\mathbf{PS})_3]^+$ complexes. Reversible transformation into neutral $[Mo_3S_4Cl_4(\mathbf{PS})_3(\mathbf{PS^*})]$ species in the presence of Cl^- anions was observed resulting in hemilabile behaviour. The equilibrium constant between cationic and neutral complexes is strongly depended on the nature of the S atom substituent. The catalytic activity of cationic complexes in the nitrobenzene reduction reflects the different hemilabile behavior of **PS1, PS2** and **PS3**.
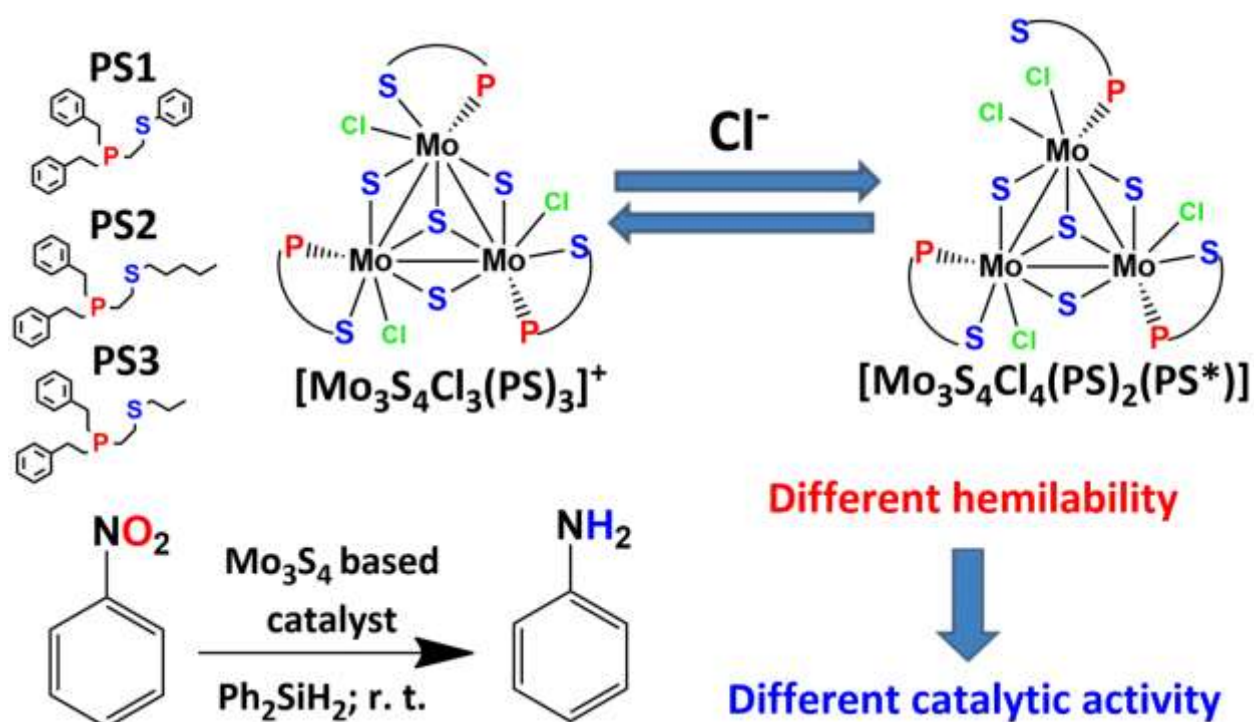
Table 1. Summary of the crystal data for compounds [**1**]$PF_6 \cdot CH_3CN$, [**1a**]$\cdot 1.6CH_2Cl_2$ and [**2**]$PF_6 \cdot 0.6CH_3CN$

Parameter	[**1**]$PF_6 \cdot CH_3CN$	[**1a**] $1.6CH_2Cl_2$	[**2**]$PF_6 \cdot 0.6CH_3CN$
Chemical formula	$C_{74}H_{84}Cl_3F_6Mo_3NP_4S_7$	$C_{73.6}H_{84.2}Cl_{7.2}Mo_3P_3S_7$	$C_{70.2}H_{100.8}Cl_3F_6Mo_3N_{0.6}P_4S_7$
M_r	1843.89	1824.95	1809.58
Crystal system, space group	Triclinic, $P\bar{1}$	Monoclinic, $C2/c$	Triclinic, $P\bar{1}$
a, b, c (Å)	12.2513 (8), 12.3807 (9), 27.167 (2)	43.9893 (15), 16.6109 (4), 24.8560 (9)	14.068 (2), 17.495 (3), 17.618 (3)
α, β, γ (°)	82.994 (3), 89.774 (2), 77.908 (3)	90, 115.229 (2), 90	90.424 (3), 105.595 (3), 99.817 (4)
V (Å^3)	3998.1 (5)	16429.8 (9)	4108.9 (10)
Z	2	8	2
μ (mm^{-1})	0.88	0.96	0.86
Crystal size (mm)	$0.20 \times 0.14 \times 0.08$	$0.22 \times 0.20 \times 0.10$	$0.22 \times 0.12 \times 0.08$
Diffractometer	Bruker Apex Duo	Bruker X8Apex	Bruker Apex Duo
T_{min}, T_{max}	0.543, 0.743	0.545, 0.742	0.565, 0.746
No. of measured, independent and observed [$I > 2\sigma(I)$] reflections	60053, 16593, 12779	45845, 18801, 11618	34957, 18768, 13909
R_{int}	0.045	0.079	0.036
θ values (°)	θ_{max} = 26.6, θ_{min} = 0.8	θ_{max} = 27.5, θ_{min} = 1.0	θ_{max} = 28.2, θ_{min} = 1.6
$(\sin \theta/\lambda)_{max}$ (Å^{-1})	0.630		0.665
Range of h, k, l	$-15 \le h \le 14$, $-15 \le k \le 15$, $-34 \le l \le 34$	$-42 \le h \le 57$, $-21 \le k \le 21$, $-32 \le l \le 29$	$-18 \le h \le 18$, $-22 \le k \le 23$, $-23 \le l \le 23$
$R[F^2 > 2\sigma(F^2)]$, $wR(F^2)$, S	0.052, 0.139, 1.06	0.075, 0.222, 1.03	0.093, 0.255, 1.03
No. of reflections, parameters, restraints	16593, 851, 12	18801, 822, 85	18768, 841, 30
Weighting scheme	$w = 1/[\sigma^2(F_o^2) + (0.0622P)^2 + 10.9909P]$ where $P = (F_o^2 + 2F_c^2)/3$	$w = 1/[\sigma^2(F_o^2) + (0.1078P)^2 + 127.820P]$ where $P = (F_o^2 + 2F_c^2)/3$	$w = 1/[\sigma^2(F_o^2) + (0.0875P)^2 + 81.7326P]$ where $P = (F_o^2 + 2F_c^2)/3$
$\Delta\rho_{max}, \Delta\rho_{min}$ (e Å^{-3})	1.87, -0.87	2.20, -1.63	4.32, -1.82

Computer programs: *APEX2* (Bruker-AXS, 2004), *SAINT* (Bruker-AXS, 2004), *SHELXS2014* (Sheldrick, 2014), *SHELXL2014* (Sheldrick, 2014), ShelXle (Hübschle, 2011), CIFTAB-2014 (Sheldrick, 2014).

Table 2. Selected bond distances (Å)* for compounds [**1**]PF$_6$·CH$_3$CN, [**1a**]·1.6CH$_2$Cl$_2$ and [**2**]PF$_6$·0.6CH$_3$CN

Distance	[**1**]PF$_6$·CH$_3$CN	[**1a**]·1.6CH$_2$Cl$_2$	[**2**]PF$_6$·0.6CH$_3$CN
Mo-Mo	2.7670(6) – 2.7718(5)	2.7540(10) – 2.8145(9)	2.7614(9) – 2.7850(9)
Mo-(μ_3-S)	2.3554(11) – 2.3604(11)	2.356(2) – 2.3810(18)	2.361(2) – 2.367(2)
Mo-(μ_2-S)	2.2916(12) – 2.3000(12)	2.270(2) – 2.3139(19)	2.296(2) – 2.320(2)
Mo-P	2.5529(13) – 2.5599(13)	2.528(2) – 2.603(2)	2.546(2) – 2.567(2)
Mo-S$_{lig}$	2.6030(13) – 2.6529(12)	2.644(2) – 2.657(2)	2.595(2) – 2.619(2)

*Standard deviations are given in brackets

Table 3. GC data for nitrobenzene reduction to aniline catalyzed by [**1**]PF$_6$ and [**2**]PF$_6$[a]

Entry	Catalyst	Solvent	T (°C)	Time (h)	Conversion (%)[b]	Yield (%)[b]
1	[**1**]PF$_6$	CH$_3$CN	25	16	>99	83
2	[**1**]PF$_6$	CH$_3$CN	80	2	94	89
3	[**1**]PF$_6$	CH$_3$CN	80	16	>99	>99
4	[**2**]PF$_6$	CH$_3$CN	25	16	79	33

[a] Reaction conditions: nitrobenzene (0.1 mmol); Ph$_2$SiH$_2$ (3.5 equiv.); catalyst (5 mol %); solvent (2 ml). [b] Determined by GC with anisole as an internal standard.